Quantitative Measurement of Illumination Invariance for Face Recognition Using Thermal Infrared Imagery*

Lawrence B. Wolff‡ Diego A. Socolinsky† Christopher K. Eveland‡

‡Equinox Corporation
9 West 57th Street
New York, NY 10019

†Equinox Corporation
207 East Redwood Street
Baltimore, MD 21202

{wolff,diego,eveland}@equinoxsensors.com

Abstract

A key issue for face recognition has been accurate identification under variable illumination conditions. Conventional video cameras sense reflected light so that image gray values are a product of both intrinsic skin reflectivity and external incident illumination, obfuscating intrinsic reflectivity of skin. It has been qualitatively observed that thermal imagery of human faces is invariant to changes in indoor and outdoor illumination, although there never has been any rigorous quantitative analysis to confirm this assertion published in the open literature. Given the significant potential improvement to the performance of face recognition algorithms using thermal infrared imagery, it is important to quantify observed illumination invariance and to establish a solid physical basis for this phenomenon. Image measurements are presented from two of the primarily used spectral regions for thermal infrared; 3-5 micron MidWave InfraRed (MWIR) and the 8-14 micron LongWave InfraRed (LWIR). All image measurements are made with respect to precise blackbody ground-truth. Radiometric calibration procedures for two different kinds of thermal IR sensors are presented and are emphasized as being an integral part to data collection protocols and face recognition algorithms.

1. Introduction

The potential for illumination invariant face recognition using thermal IR imagery has been recognized in the past [8, 9, 12]. This invariance can be qualitatively observed in Figure 1 for a co-registered LWIR and visible video camera sequence of a face under three different illumination conditions. For this sequence a single 60 Watt light bulb mounted in a desk lamp illuminates a face in an otherwise completely dark room and was moved into different positions. The top row of visible video imagery shows dramatic changes in the appearance of the face and it is well known that this typically confounds face recognition algorithms [11, 1]. The middle row shows LWIR imagery which unlike its co-registered visible counterpart appears to be remarkably invariant across different illuminations, except in the image area corresponding to the glasses. The bottom row demonstrates the invariance of LWIR imagery by visualizing both visible and LWIR fused together as intensity and color-hues respectively. While intensity is variable from one illumination condition to another, color hue remains mostly invariant. As we will see, illumination invariance in the thermal IR while not being completely ideal is nonetheless strongly approximated.

As a result of recent efforts by the authors, a multi-modal database of over 100 face images has been obtained simultaneously for visible, SWIR, MWIR and LWIR using the camera setup shown in Figure 2. Collection of image data was repeated for three different illumination conditions, i) Frontal, ii) Frontal-Left, iii) Frontal-Right, using standard 3200 Deg. K color temperature photographic bulbs. Performance for two mainstream face recognition algorithms was directly compared on various subsets of co-registered visible and LWIR imagery for different illuminations [4]. The performance of these algorithms on LWIR imagery was consistently better than for visible imagery, indirectly supporting the assertion that thermal IR face imagery is illumination invariant. Although an initial set of results of ongoing experimentation this set of performance results gives hard evidence that face recognition using thermal IR has a consistent performance advantage over conventional video in variable illumination environments.

*This research was supported by the DARPA Human Identification at a Distance (HID) program under contract# DARPA/AFOSR F49620-01-C-0008.

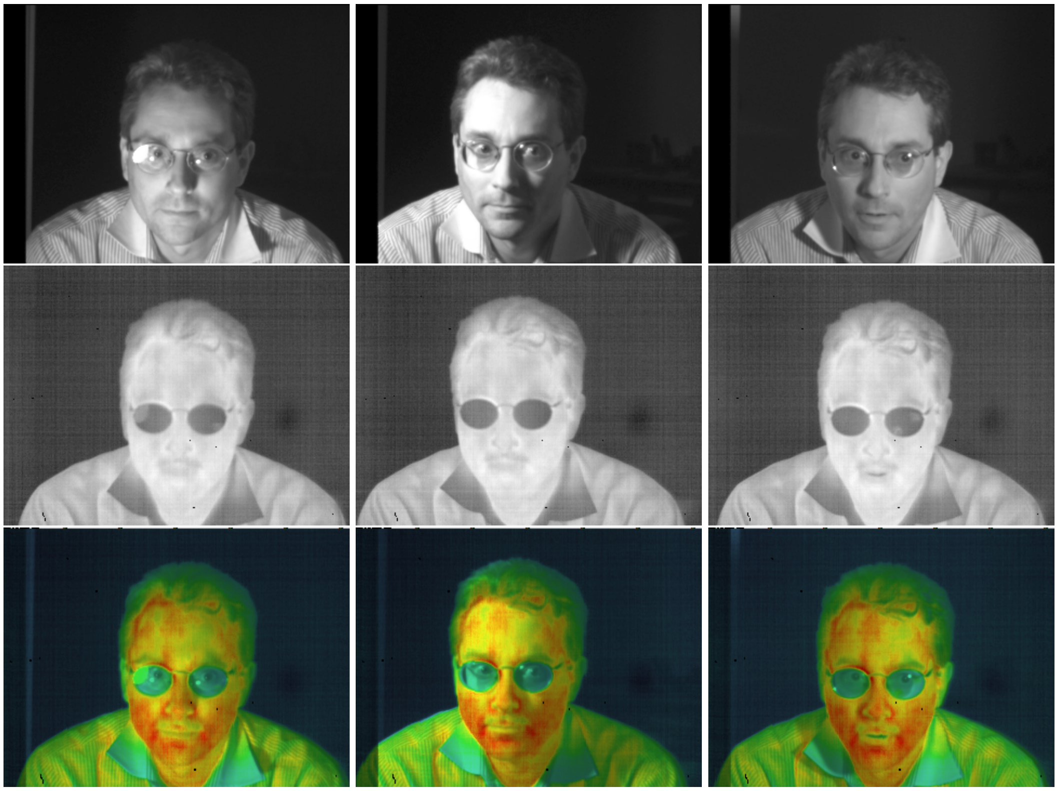

Figure 1. A qualitative demonstration of the illumination invariance for LWIR imagery of a face under different illuminations. TOP ROW: Visible imagery of a face under three illumination conditions respectively Front, Left and Right, MIDDLE ROW: Co-registered thermal IR imagery simultaneously acquired for each of the three images in top row respectively, BOTTOM ROW: complete visible/thermal IR fusion showing a color thermal map superimposed on the visible features of the face.

In this paper we delve deeper into physical phenomenology to more directly analyze illumination invariance of faces in the thermal IR. The objectives are three-fold:

- Establish image data collection procedures enabling a rigorous way to quantify illumination invariance of the human face in both the MWIR and LWIR.
- Directly compare radiometrically calibrated MWIR and LWIR face imagery under different illumination with inter-personal face variations and noise characteristics of the thermal IR sensors.
- Find a physical basis for the MWIR/LWIR illumination invariance of human faces.

These are believed to be an important foundation for the development of face recognition algorithms in the thermal IR. Up until now, face recognition algorithms have been developed almost exclusively under the assumption of visible video. Thermal IR imagery has many advantages because it measures different phenomenology, and these advantages cannot be fully harnessed unless the phenomenology is well understood.

2. Blackbody Radiation and Emissivity

All objects above absolute zero temperature emit electromagnetic radiation. In the early 1900s Planck was the first to characterize the spectral distribution of this radiation for a *blackbody*, which is an object that completely absorbs electromagnetic radiation at all wavelengths [10]. The quantitative expressions for this spectral distribution in different units of energy are given by equations 1 and 2 in the next section. Only very few objects are perfect energy absorbers, particularly at all wavelengths. The proportional amount of energy emission with respect to a perfect absorber is called the *emissivity*, $\epsilon(T, \lambda, \psi)$, which takes values in the range $[0, 1.0]$. In addition to temperature T, and, wavelength λ, this can also be a function of emission angle ψ. Kirchoff's law states that the emissivity at a point on an object is equal

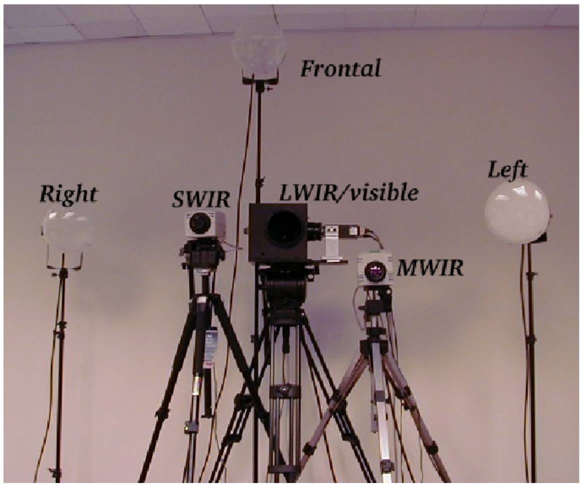

Figure 2. Camera and illumination equipment set-up used for simultaneous data collection of visible, SWIR, MWIR and LWIR imagery.

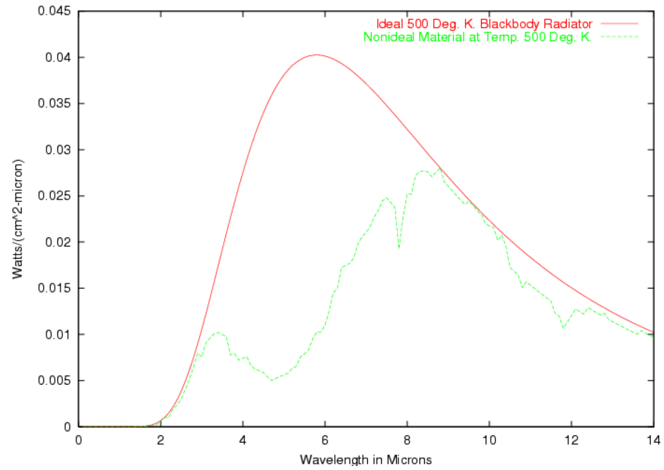

Figure 3. Comparison of an ideal blackbody Planck curve with a nonideal emitter at the same temperature.

to the *absorption*, $\alpha(T, \lambda, \psi)$, namely:

$$\epsilon(T, \lambda, \psi) \; = \; \alpha(T, \lambda, \psi) \; .$$

This is a fundamental law that effectively asserts the conservation of energy. Blackbody objects are therefore the most efficient radiators, and for a given temperature T emit the most energy possible at any given wavelength. Figure 3 compares the spectral distribution of the emission of an ideal blackbody at 500 degrees Kelvin (227 degrees Centigrade) with that of a nonideal emitter (e.g., could be a piece of bare metal) also at the same temperature. In this case the nonideal emitter has low emissivity at wavelengths in the MWIR spectral region (3-5 microns) and generally good emissivity in the LWIR spectral region (8-14 microns).

Under most practical conditions, 2-D imaging array thermal IR sensors (i.e., what are termed *staring arrays*) measure simultaneously over broadband wavelength spectrums, as opposed to making measurements at narrow almost monochromatic wavelengths (e.g., an IR spectrophotometer which measures only one point in a scene). With a staring array sensor it is possible to measure *average emissivity* over a broadband spectrum (e.g., 3-5 microns, 8-14 microns), which in Figure 3 is simply the ratio of the area under the nonideal curve to the area under the Planck curve over the respective wavelength spectrum.

Using terminology adapted from the computer vision literature emissivity is a *thermal albedo* which is complementary to the more familiar reflectance *albedo* [6, 7]. For instance a Lambertian reflector can appear white or grey depending on its efficiency for reflecting light energy. The more efficient it is in reflecting energy (more reflectance albedo) the less efficient it is in thermally emitting energy respective to its temperature (less thermal albedo). Many materials that are poor absorbers transmit most light energy while reflecting only a small portion. This applies to a variety of different types of glass and plastics in the visible spectrum.

Some of these principles can be observed in Figure 1. Plastic materials transparent in the visible spectrum that compose glasses are opaque in the LWIR and appear dark. Emissivity of this material is small in the visible spectrum while being significantly above 0.80 in the MWIR and LWIR spectral regions. The dark appearance of glasses in the LWIR and the MWIR relative to thermal emission from human facial skin is mostly due to the glasses being close to room temperature about 15 deg. C cooler than body temperature. We performed simple experiments whereby these same pair of glasses were heated close to body temperature. Sure enough the glasses appeared thermally much brighter, but not as much thermal emission as facial skin at the same temperature. Also, from Figure 1 the influence of reflection of external illumination from glasses is far more prominent than that from facial skin. All this initially suggests that facial skin has very high emissivity significantly higher than that of the material comprising glasses. A quantitative estimate of the average emissivity of facial skin in the MWIR and LWIR is developed in Section 4 supporting this assertion.

3. Calibration of Thermal IR sensors

Just like visible video cameras, thermal IR cameras measure energy of electromagnetic radiation, the main differ-

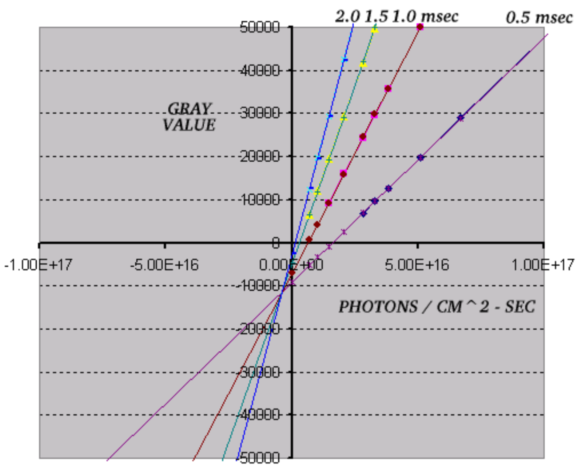

Figure 4. Responsivity curves for different integration times for the Indigo Merlin Series MWIR camera used for collecting image data presented in this paper.

ence being that because thermal IR cameras sense at such long wavelengths, they measure radiation that has been typically thermally emitted from anything above room temperature or even colder. Of course visible cameras see radiation emitted from very hot sources (e.g., the sun or artificial light bulbs which are thousands of degrees Kelvin) but the primary scene elements of interest in the visible are objects from which such light is reflected. Sometimes there is the misconception that thermal IR cameras directly measure temperature, which would be true if all objects were blackbodies. Temperature can be determined indirectly from a thermal IR camera by measurement of energy of emitted radiation, using precise knowledge of emissitivity of the object, which is dependent upon a number of parameters.

Thermal IR cameras can be radiometrically calibrated using a blackbody ground-truth source. Radiometric calibration achieves a direct relationship between the grey value response at a pixel and the absolute amount of thermal emission from the corresponding scene element. This relationship is called *responsivity*. Depending on the type of thermal IR camera being used, thermal emission flux is measured in terms of $Watts/cm^2$ or $Photons/(cm^2 - second)$ [3]. The grey value response of pixels for a MWIR camera with an Indium Antimonide (InSb) focal plane array is linear with respect to $Photons/(cm^2 - second)$. The grey value response of pixels for an LWIR camera using a microbolometer focal plane array is linear with respect to $Watts/cm^2$. *Two-point radiometric calibration* uses a blackbody plate filling the field of view of the thermal IR camera and capturing images for the blackbody at two different temperatures. Given that human body temperature is 37 deg. C, two good temperatures to use for calibrating the imaging of humans in a room temperature scene would be 20 deg. C and 40 deg. C (293 deg. K and 313 deg. K). According to Planck's law, the spectral distribution of a blackbody is given by:

$$W(\lambda, T) = \frac{2\pi hc^2}{\lambda^5(e^{\frac{hc}{\lambda kT}} - 1.0)} \quad [Watts/cm^2]\mu m^{-1} \quad (1)$$

$$Q(\lambda, T) = \frac{2\pi c}{\lambda^4(e^{\frac{hc}{\lambda kT}} - 1.0)} \quad [Photons/cm^2 - sec]\mu m^{-1} \quad (2)$$

which are equivalently expressed in each unit of energy flux. For completeness h is Planck's constant, k is Boltzmann's constant, T is absolute temperature and λ is wavelength. See [10] for details. Since absolute thermal emission is known by computing the area under the Planck curve for the corresponding temperature and wavelength spectrum, a responsivity line is generated at each pixel by two (grey-value, thermal emission) coordinate values. The slope of this responsivity line is called the 'gain' and the vertical translation of the line is 'offset'. The gain and offset for each pixel on a thermal IR focal plane array can be significantly variable across the array. Radiometric calibration standardizes thermal emission measurement by generating a responsivity line for each pixel.

Figure 4 shows responsivity lines respective to different integration times, for a single pixel near the center of a MWIR InSb focal plane array that was used to collect face imagery. Eight different temperatures of a blackbody were used to generate multiple data points demonstrating the highly linear response. It is clearly important to record all thermal IR camera parameters for a given radiometric calibration. Note that the responsivity lines for different integration times intersect at the same point, related to various DC bias control settings on the camera. Beyond camera parameters, if a MWIR or LWIR camera is originally radiometrically calibrated in an indoors environment, taking it outdoors where there is a significant ambient temperature difference, the gain and offset of linear responsivity of focal plane array pixels will change as optical lens temperature in front of the focal plane array changes. Radiometric calibration standardizes all thermal IR data collections, whether they are taken under different environmental factors or with different thermal IR cameras or at different times.

4. Measuring Illumination Invariance

With the equipment set-up shown in Figure 2, 40 image frame sequences of visible, SWIR, MWIR and LWIR were digitized simultaneously at 10 frames/second (i.e., 4 seconds duration), while a human subject was reciting the vowels ’a’, ’e’, ’i’, ’o’, ’u’. This creates a continuous image sequence with changes in expression throughout providing significant intra-personal variation over the course of multiple frames. At the same time there is little facial movement between consecutive image frames 1/10 second apart allowing for analysis of image variations due to sensor noise. For a given human subject three 40 image frame sequences were acquired respective to i) Frontal light source on, ii) Frontal and Left light source on, and, iii) Frontal and Right light source on.

Prior to data collection, the radiometric calibration procedure described in the previous section was performed for the Indigo Merlin series MWIR and LWIR cameras using a model 350 Mikron blackbody source. Software was developed to convert raw MWIR and LWIR image grey values directly into respective thermal emission values from groundtruth blackbody images. Raw image grey values for the MWIR and LWIR cameras are 12-bit integers from which floating point thermal emission values were computed and then rounded back to 12-bit values with appropriate dynamic range.

Variation in illumination is one of the biggest factors that confounds face recognition algorithms in the visible spectrum. In the thermal IR, changes in illumination appear to play less of a role, but how does one quantify this invariance in terms that are meaningful to face recognition ? One way is to quantitatively compare the effect that variation in illumination has on face images in the thermal IR with other factors that contribute to changes in face imagery, such as variations in facial expression and more subtle variations due to camera noise.

Figure 5 shows simultaneously acquired MWIR and LWIR images that have been radiometrically calibrated, together with corresponding grey value histograms of an individual under the three illumination conditions previously described. These images are the 3rd image frame out of each respective 40 image frame sequence. Grey values in the histograms are represented as 16-bit integers with the high 12-bits being the actual image grey value. The grey level histograms are remarkably stable across different illuminations for both the MWIR and the LWIR images. Of the variations that are present in the respective histograms, which are due to change in illumination and which are due to other factors ? For instance note the darker mouth region in the MWIR image for Right illumination as compared to the mouth region in the MWIR images for other illuminations. The darker mouth region is due to the subject breathing in room temperature air at the moment cooling down the mouth. This has nothing to do with any illumination condition.

The histograms in Figure 5 can be compared with those in Figure 6, which shows the grey value histograms corresponding to the 4th and 20th image frame out of the 40 image frame sequence respective to the Frontal illumination condition. In this case, illumination is the same but the 4th frame being consecutive with the 3rd frame isolates changes due to camera noise, and the 20th frame occuring just under two seconds later means the subject has changed facial expression. The variations in the grey level histogram due to camera noise and to different facial expression under same illumination are of similar magnitude to variations occurring under different illumination.

A quantitative analysis of invariance in the framework of hypothesis testing was also performed. For each video sequence in our database, the locations of the subject’s pupils and frenulum were semi-automatically located. Using these coordinates, normalized images of the subject’s face were extracted so that left and right pupils are placed at fixed coordinates. Figure 7 shows examples of the normalized faces for front- and left-illuminated visible and LWIR images. Note that these images contain a minimal number of background pixels. The following analysis is repeated for two different distance measures between images. Firstly we consider the L^2 distance between normalized images taken as vectors. Secondly, we use the Kullback-Leibler divergence[1] between the histograms of the normalized faces, given by

$$I(P,Q) = \int P \, \log \frac{P}{Q},$$

where P and Q are the respective normalized histograms.

For each video sequence of $40 + 3$ frames, we compute the $43 \cdot 42/2 = 903$ distances between normalized faces for distinct pairs of frames. Also, we compute the $43 \cdot 43 = 1849$ distances between normalized faces for sequences of the same subject and modality, one sequence with frontal illumination and the other with lateral illumination. From these computations we estimate (non-parametrically) the distribution of distances for images with the same illumination condition and with different illumination conditions. Figures 8, 9, 10 and 11 show the estimated distributions for the L^2 distance and KL-divergence for two subjects in our database. With an infinite supply of images, we would expect the distances to behave according to a χ distribution with the number of degrees of freedom matching the number of pixels in the normalized faces, and indeed the experimental estimates approximate χ distributions.

It is clear from Figures 8, 9, 10 and 11 that the distances between normalized visible faces with different illumination conditions are much larger than those for visible faces with the same illumination condition. This indicates that the variation in appearance due to change in illumination is much larger than that due to change in facial expression. The corresponding statement for LWIR imagery does not

[1]The Kullback-Leibler divergence does not satisfy the triangle inequality, and thus is not strictly a distance. However, it provides an information-theoretic measure of similarity between probability distributions.

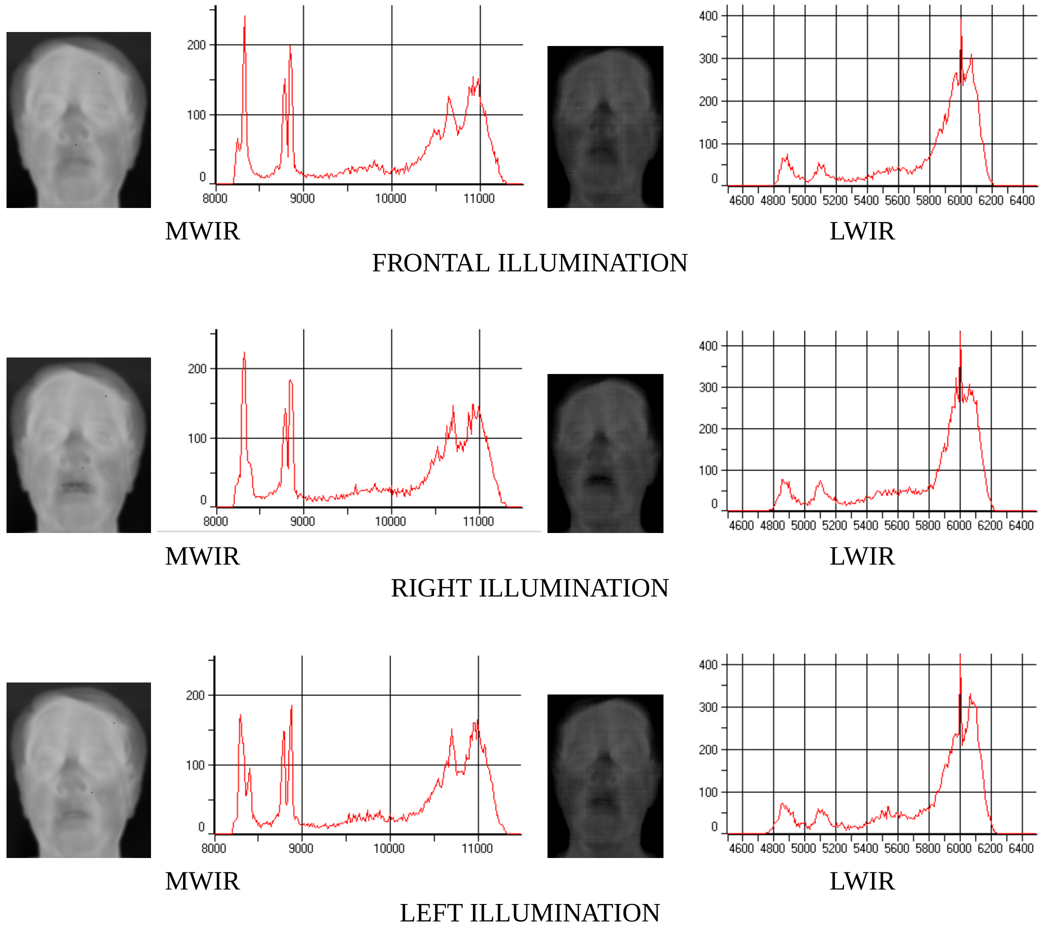

Figure 5. MWIR and LWIR imagery of a face for three illumination conditions and respective histograms of the 3rd frame out of a sequence of 40 images.

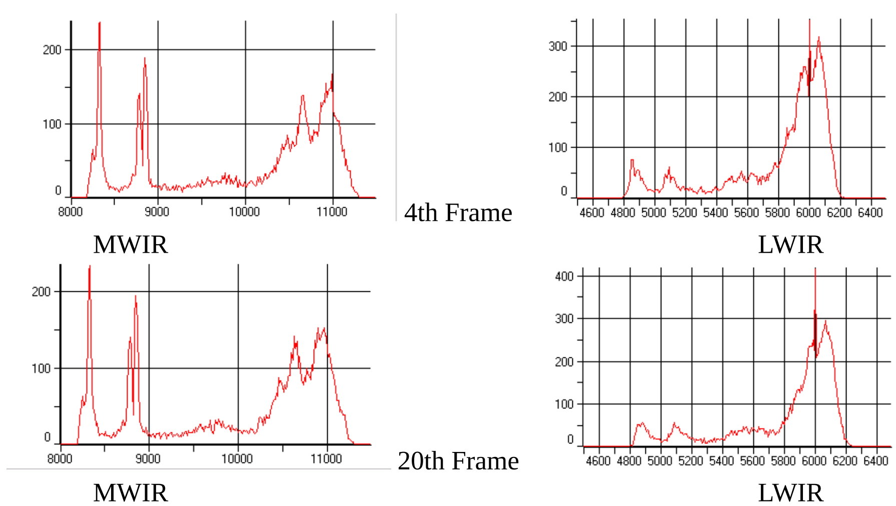

Figure 6. MWIR and LWIR imagery of the same face as Figure 5 respective to frontal illumination for the 4th frame (TOP ROW) and 20th frame (BOTTOM ROW) out of a sequence of 40 images.

Figure 7. Example of visible (top) and LWIR (bottom) normalized face images.

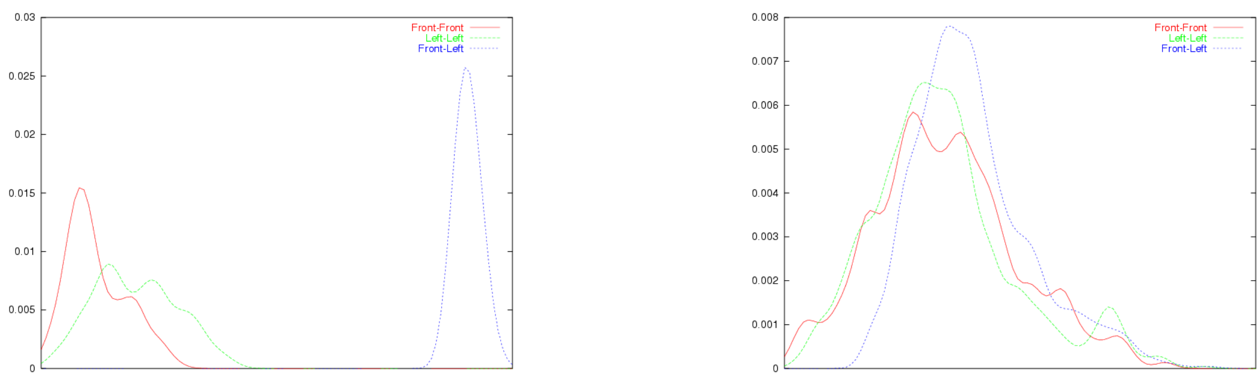

Figure 8. Distribution of L^2 distances for visible (left) and LWIR (right) images of subject 2344.

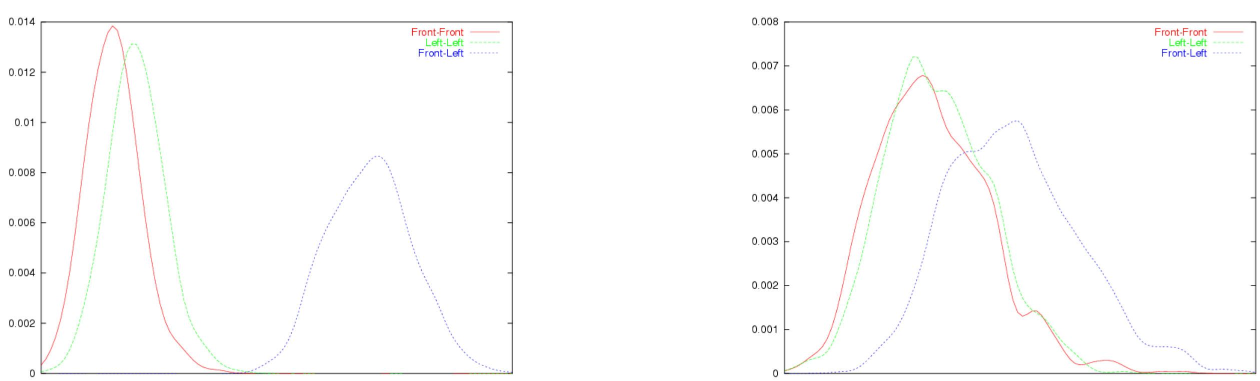

Figure 9. Distribution of Kullback-Leibler divergences for visible (left) and LWIR (right) images of subject 2344.

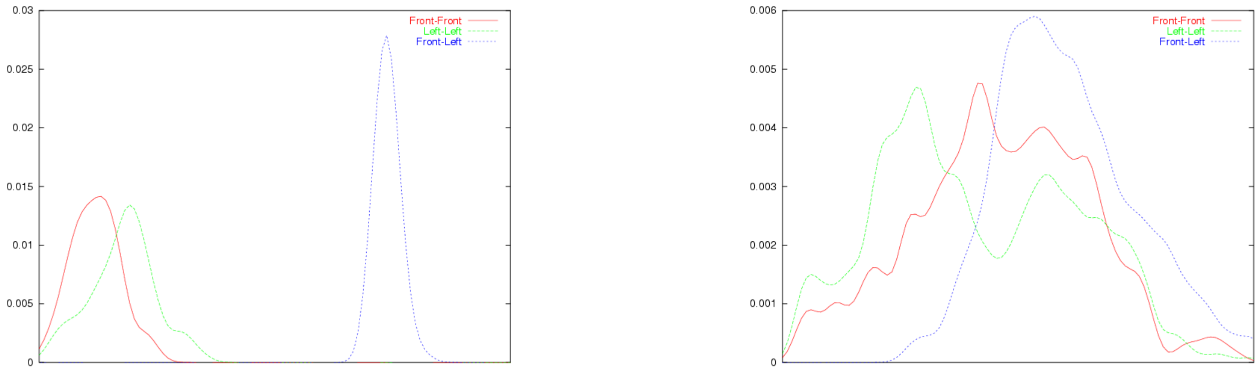

Figure 10. Distribution of L^2 distances for visible (left) and LWIR (right) images of subject 2413.

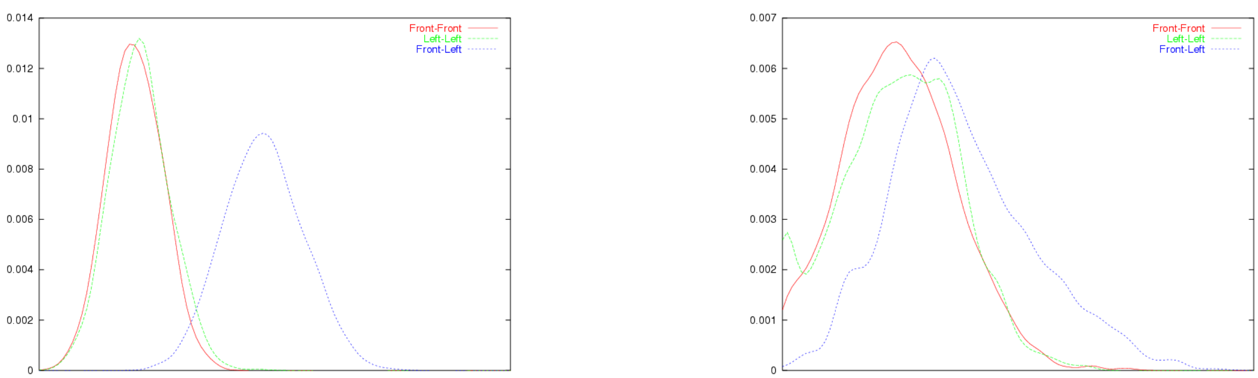

Figure 11. Distribution of Kullback-Leibler divergences for visible (left) and LWIR (right) images of subject 2413.

hold. That is, looking once again at Figures 8, 9, 10 and 11, one can see that the distribution of distances between normalized faces with different illumination conditions is comparable (but not equal, see below) to the distribution obtained by using images acquired with the same illumination condition. In other words, the variation in appearance introduced by changes in illumination and expression is comparable to that induced by changes in facial expression alone. Phrasing these statements as formal hypothesis, we can reject the null-hypothesis of illumination invariance for visible imagery with a p-value smaller than 0.01, whereas we are unable to reject the null-hypothesis for LWIR imagery. The slight shift in the distributions to the right for variable illumination suggests that illumination invariance in the LWIR is not completely ideal.

5. Emissivity of Human Facial Skin

One plausible reason why human faces are strongly illumination invariant in the thermal IR is that there may simply be little illumination from common sources in this spectral region in the first place. For the LWIR this is immediately discounted by the observed prominent reflection of a light bulb in the pair of glasses in Figure 1. This is also observed in the MWIR.

Figure 12 shows a comparison of blackbody spectral distributions at various temperatures, corresponding to different common sources of illumination and human skin. As mentioned above, the color temperature of the photographic light bulbs used for data collection is 3200 deg. K and while this is a measure of *correlated* color temperature projected onto the Planckian locus on the CIE color chart, the Planck distribution is still a good approximation [13]. For reasons determined below an upper bound on the amount of thermal emission from skin at different wavelengths is the Planck distribution at 34.3 deg. C (307.3 deg. C). Figure 12 shows that the amount of thermal emission from a common light bulb is three to four orders of magnitude greater than the thermal emission from skin in both the 3-5 micron MWIR region and the 8-14 micron LWIR region. Empirical observation with our own MWIR and LWIR cameras showed that direct illumination from an incandescent filament through lightbulb glass and plastic diffuser is at least 300 times greater than thermal emission from human facial skin. This is a rather striking fact given that thermal IR imagery of faces is highly illumination invariant. Human skin must absorb a large quantity of radiation in both the MWIR and the LWIR implying that skin has very high emissivity.

For completeness, the thermal emission of two common natural outdoor sources of illumination is also characterized in Figure 12. The spectral output of the Sun is well approximated by a 5500 deg. K. [10] Planck curve which in the MWIR and LWIR shows about a factor of two greater thermal emission than for indoor artificial illumination. This will challenge the illumination invariance of faces in the thermal IR a little more than for indoor illumination, and points to an important topic of future experimentation with outdoor data collection of thermal IR imagery. Compared to the Sun, other outdoor sources of illumination in the thermal IR are negligible. The scattering of light from the atmosphere is extremely inefficient for longer wavelengths according to the Rayleigh $1/\lambda^4$ Law [2], and is virtually non-existent for the thermal IR. Thermal IR radiation from the sky does exist in the form of thermal emission from the surrounding atmosphere which has a computed average absolute temperature of 258 Deg. K [5]. The Planck curve for this temperature is shown as an upper bound on thermal emission from sky and is one to two orders of magnitude smaller than thermal emission from skin.

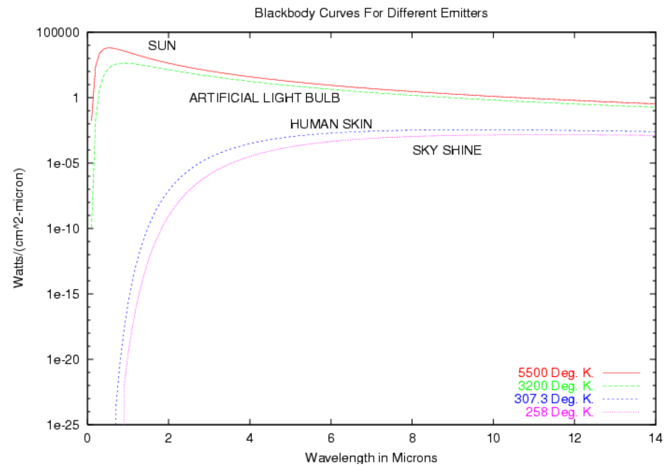

Figure 12. Blackbody Planck curves comparing thermal IR emission from common natural and artificial illumination sources to thermal IR emission from human skin.

Figure 13 shows a human subject in the same scene with a 6”x6” square blackbody (Mikron model 345) imaged in the MWIR and LWIR spectrums. Separate images are taken for the blackbody at two different temperatures: 32 deg. C and 35 deg. C. The corresponding histograms show grey value modes for the facial skin image region and for the blackbody image region. Prior to imaging, an Anritsu thermocouple was used to make contact temperature measurements on the forehead, on both cheeks and on the chin of the human subject. An average skin surface temperature of 32 deg. C was observed. Note however that the face thermally emits more energy than does a 32 deg. C blackbody. This is a physical contradiction unless radiation emitted from below the skin surface (as high as 37 deg. C internal body temperature) also contributes. This may reveal an important aspect of how thermal emission arises from human anatomy and perhaps even a physical mechanism for why skin has such high absorption in the thermal IR. Evidently skin layers must be significantly transmissive to thermal emission from underlying internal anatomy which is at a higher temperature. This is qualitatively evidenced from thermal observation of prominent vasculature beneath the skin particularly in the neck. Just how far below the skin surface thermal emission gets transmitted is unclear and is an avenue for future research. If at least the outer layers of skin are transmissive, then incident thermal IR illumination must be first transmitted and then absorbed within deeper layers of skin or other anatomy. This may explain why the amount of thermal emission from skin seems to be independent of external skin color in the visible spectrum.

We conclude by computing a quantitative estimate of the average emissivity respective to the MWIR and the LWIR for human facial skin from the data in Figure 13. First computed is the mean thermally emitted energy of facial skin $Skin^{mean}_{energy}$. Since the thermal IR imagery used is radiometrically calibrated we can compute the mean grey value in the histogram for the facial lobe and determine the corresponding energy by linearly interpolating between the grey value peaks for the blackbody at 32 deg. C (305 deg. K) and 35 deg. C (308 deg. K) and respective blackbody energies. For the MWIR this is:

$$Skin^{mean}_{energy} \; = \; BB^{305K}_{energy} + \; [BB^{308}_{energy} - BB^{305}_{energy}] \frac{Skin^{mean}_{grey} - BBgrey^{305K}_{max}}{BBgrey^{308K}_{max} - BBgrey^{305K}_{max}} \qquad (3)$$

where

$$BB^{308K}_{energy} = \int_3^5 Q(\lambda, 308K) d\lambda$$

$$BB^{305K}_{energy} = \int_3^5 Q(\lambda, 305K) d\lambda \; .$$

For the LWIR replace $Q(\lambda, T)$ with $W(\lambda, T)$ and integration occurs over wavelengths from 8 to 14 microns.

We then make a conservative estimate of the lower bound for average emissivity, ϵ, by comparing the mean thermally emitted energy of facial skin to a blackbody at internal body temperature 37 deg. C. This yields:

$$\epsilon^{skin}_{mwir} \; > \; \frac{Skin^{mean}_{energy}}{\int_3^5 Q(\lambda, 310K) d\lambda} = 0.91$$

$$\epsilon^{skin}_{lwir} \; > \; \frac{Skin^{mean}_{energy}}{\int_8^{14} W(\lambda, 310K) d\lambda} = 0.97$$

These lower bounds are conservative as this effectively assumes that thermal emission is being sensed from a material that has a temperature of 37 deg. C throughout. In reality there is a temperature gradient from the skin surface at 32 deg. C through skin layers and blood vessels eventually to 37 deg. C internal body temperature. The *average* temperature lies somewhere between 32 and 37 deg. C. It is clear that skin at least has high emissivity in the MWIR and extremely high emissivity in the LWIR supporting a physical basis for excellent illumination invariance.

As the emissivity of skin is so close to 1.0, it is meaningful to quantify what is the average skin temperature due to the internal temperature gradient below the skin. This can be defined in terms of a *blackbody equivalent temperature of skin*, to be the temperature of a blackbody emitting equivalent energy as $Skin^{mean}_{energy}$. This temperature, $SkinBB^T$, can be computed by numerically solving the following integral equations:

$$\int_3^5 Q(\lambda, \text{SkinBB}^T_{mwir}) d\lambda = Skin^{mean}_{mwir\ energy}$$

$$\int_8^{14} W(\lambda, \text{SkinBB}^T_{lwir}) d\lambda = Skin^{mean}_{lwir\ energy} \; .$$

From the data presented in Figure 13 we compute:

$$SkinBB^T_{mwir} = 34.3 deg.C \qquad SkinBB^T_{lwir} = 34.7 deg.C.$$

6. Conclusion and Future Work

This paper has defined an initial framework for quantitatively analyzing the illumination invariance of thermal IR imagery of faces. Initial results suggest that the quantitative change to thermal IR imagery of faces due to variations in illumination are comparable but slightly greater than changes produced from variation in facial expression and temporal camera noise. We were also able to quantitatively estimate the high emissivity for human facial skin, physically supporting the strong approximation to illumination invariance. What needs to be further developed is a physical thermal model for human skin able to accurately predict observed thermal emission characteristics. An initial model suggests that the outer most layers of facial skin may be fairly translucent in the MWIR and LWIR with stronger aborption occuring in the inner skin layers and underlying tissue.

The results obtained so far have been performed on only a handful of racially and gender diverse individuals. What is needed is similar analysis over a much larger group of individuals. The current multimodal database of over 100 faces is ever growing and will soon be extended to outdoor imagery. Not addressed in this paper is illumination invariant characteristics of hair both on the head and on the face. Another issue is how to compensate for reflected illumination from glasses.

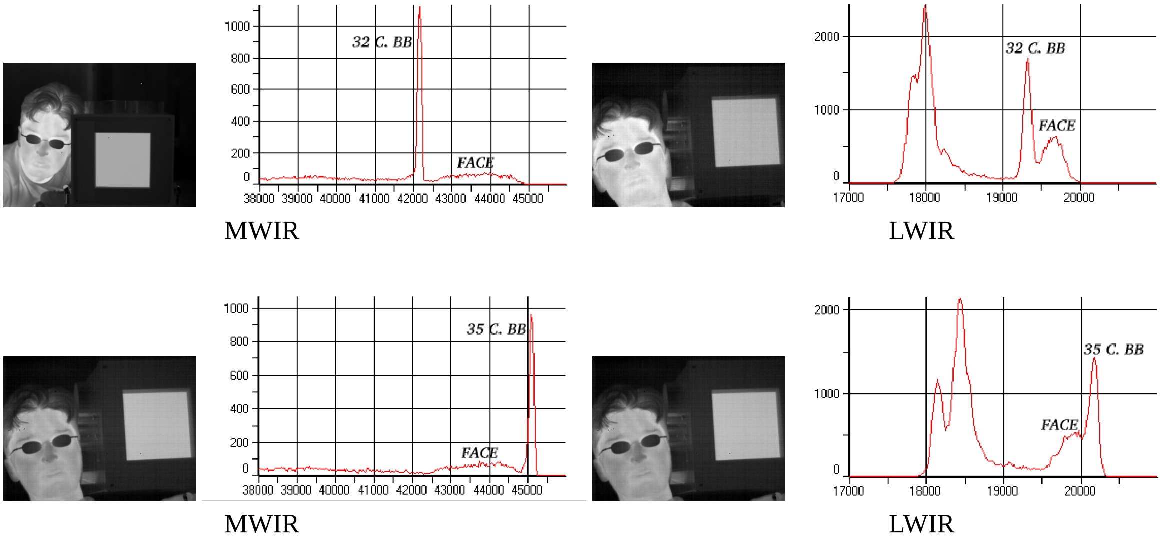

Figure 13. Direct comparison of MWIR and LWIR imagery of a face with a groundtruth blackbody at 2 different temperatures, 32 deg. C and 35 deg. C

References

[1] Yael Adini, Yael Moses, and Shimon Ullman. Face Recognition: The Problem of Compensating for Changes in Illumination Direction. *IEEE Transactions on Pattern Analysis and Machine Intelligence*, 19(7):721–732, July 1997.

[2] S. Chandrasekhar. *Radiative Transfer*. Dover Publications, New York, 1960.

[3] E.L. Dereniak and G.D. Boreman. *Infrared Detectors and Systems*. John Wiley & Sons, Inc, 1996.

[4] D.A. Socolinsky L.B. Wolff J. Neuheisal C.K. Eveland. Illumination invariant face recognition using thermal ir imagery. In *Proceedings of IEEE Conference on Computer Vision and Pattern Recognition (CVPR)*, Kauai, Hawaii, December 2001.

[5] B. Finlayson-Pitts and J. Pitts. *Chemistry of the Upper and Lower Atmosphere : Theory, Experiments, and Applications*. Academic Press, 1999.

[6] B.K.P. Horn. Understanding image intensities. *Artificial Intelligence*, pages 1–31, 1977.

[7] B.K.P. Horn and R.W. Sjoberg. Calculating the reflectance map. *Applied Optics*, 18(11):1770–1779, June 1979.

[8] I. Pavlidis and Symosek. The, Imaging Issue, in an Automatic Face/Disguise of Detection System. In *Proceedings IEEE Workshop on Computer Vision Beyond the Visible Spectrum: Methods and Applications*, Hilton Head, 2000.

[9] F. J. Prokoski. History, Current Status, and Future of Infrared Identification. In *Proceedings IEEE Workshop on Computer Vision Beyond the Visible Spectrum: Methods and Applications*, Hilton Head, 2000.

[10] R. Siegal and J.R. Howell. *Thermal Radiation Heat Transfer*. McGraw-Hill, 1981.

[11] M. Turk and A. Pentland. Eigenfaces for Recognition. *J. Cognitive Neuroscience*, 3:71–86, 1991.

[12] Joseph Wilder, P. Jonathon Phillips, Cunhong Jiang, and Stephen Wiener. Comparison of Visible and InfraRed Imagery for Face Recognition. In *Proceedings of 2nd International Conference on Automatic Face & Gesture Recognition*, pages 182–187, Killington, VT, 1996.

[13] G. Wyszecki and W. S. Stiles. *Color Science : Concepts and Methods, Quantitative Data and Formulae*. Wiley Series in Pure and Applied Optics, 1981.